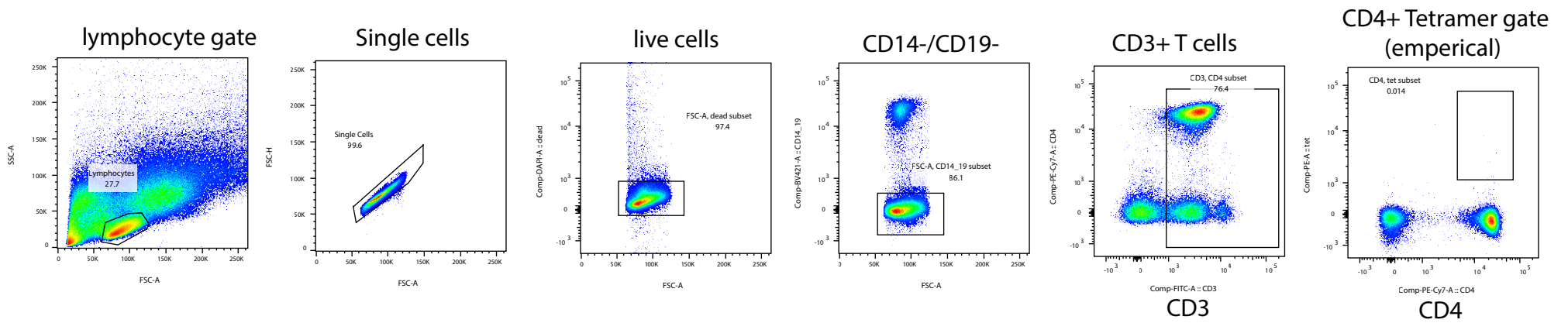
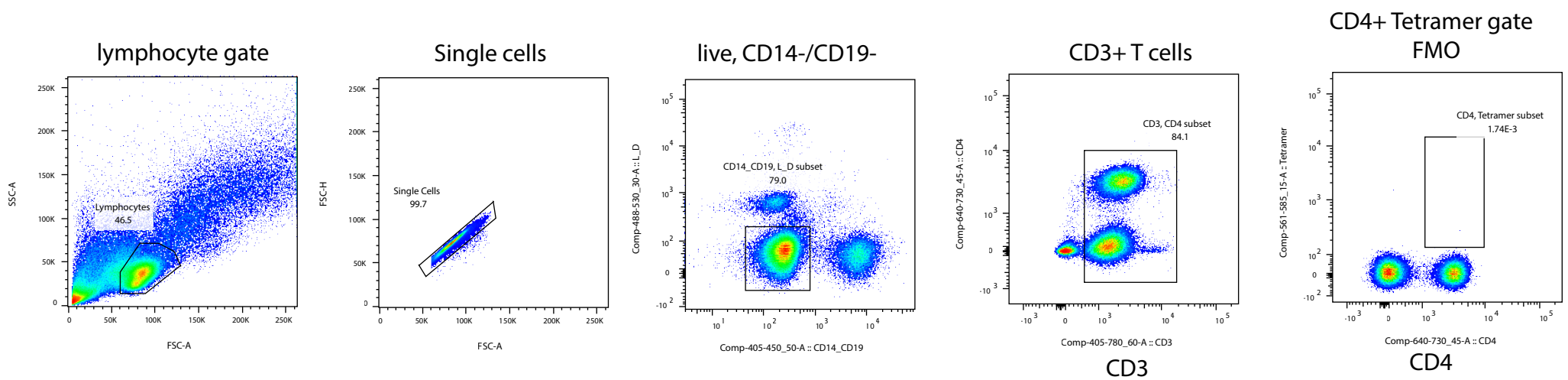


a

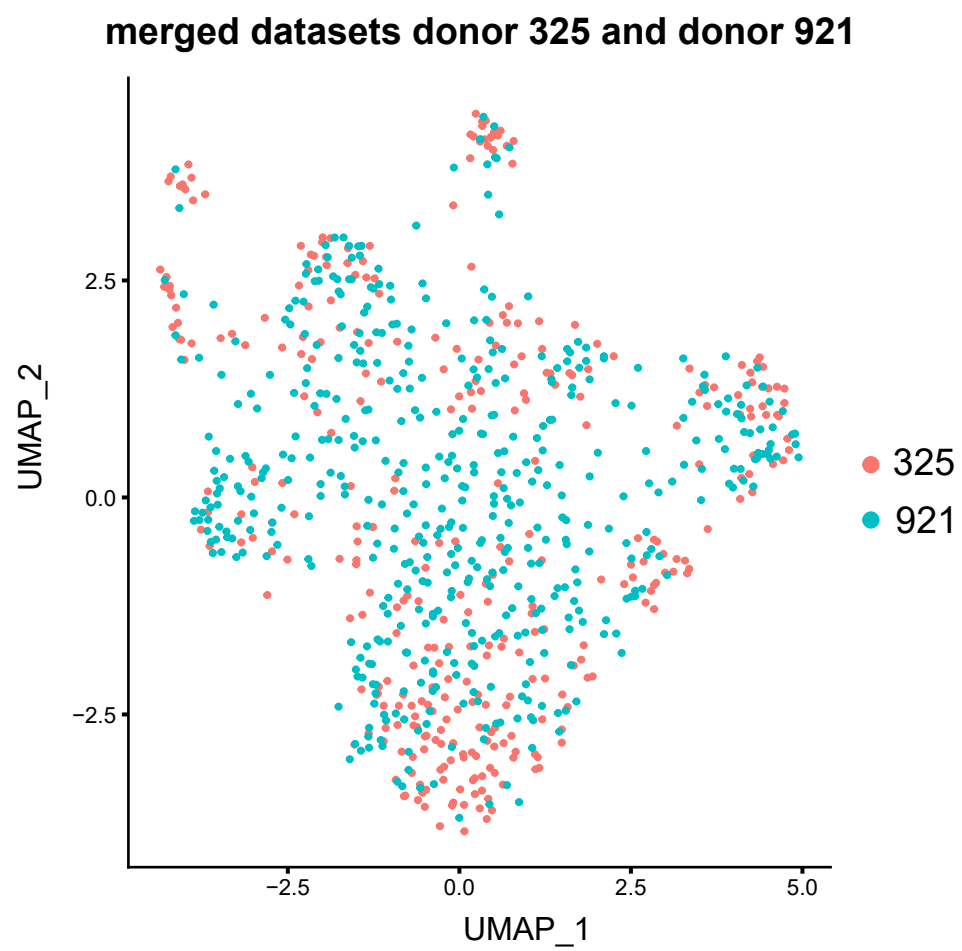


b

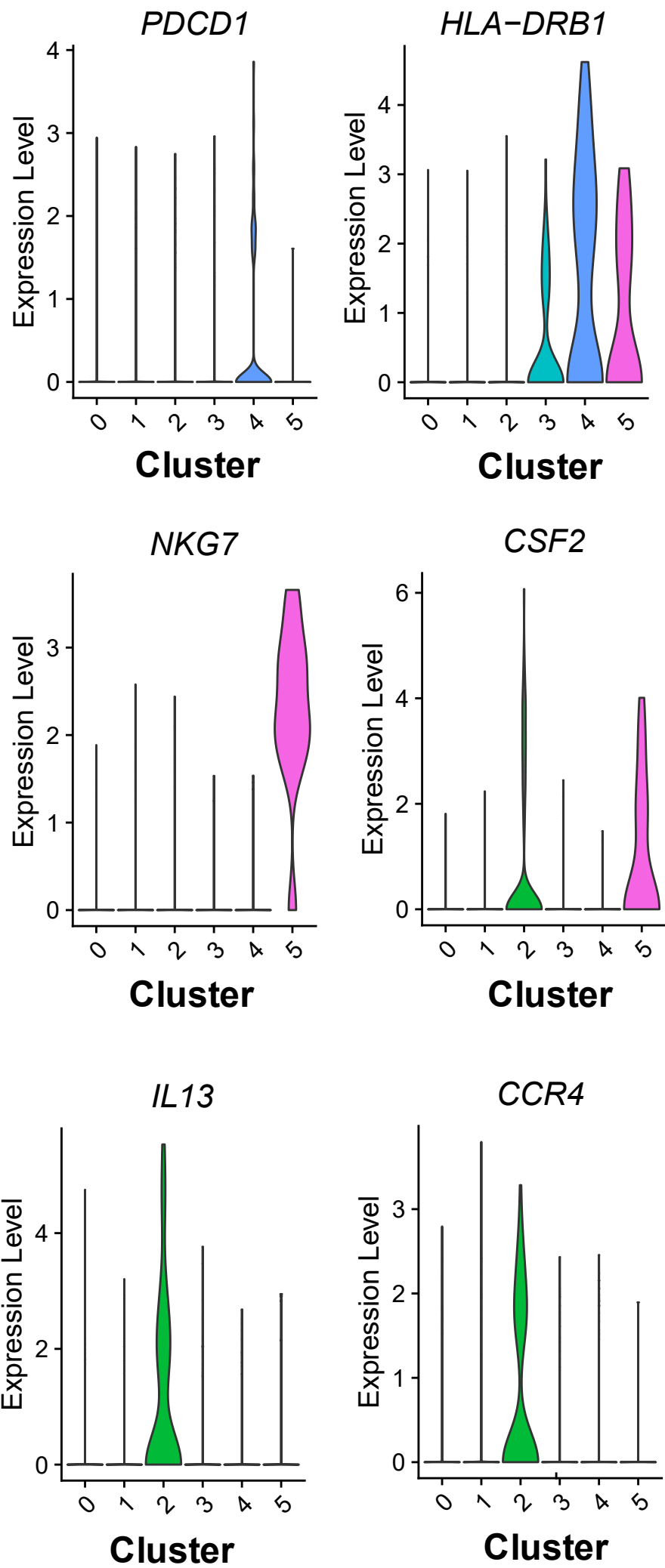


Supplementary Figure 1. Gating trees for ex vivo CD1a tetramer stainings.

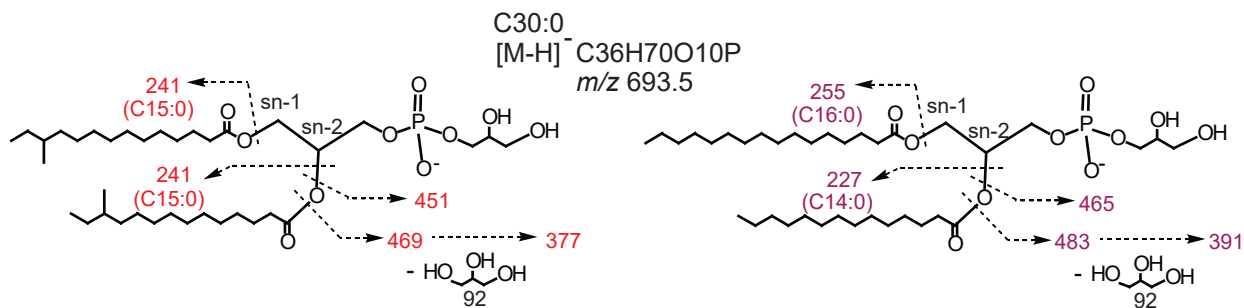
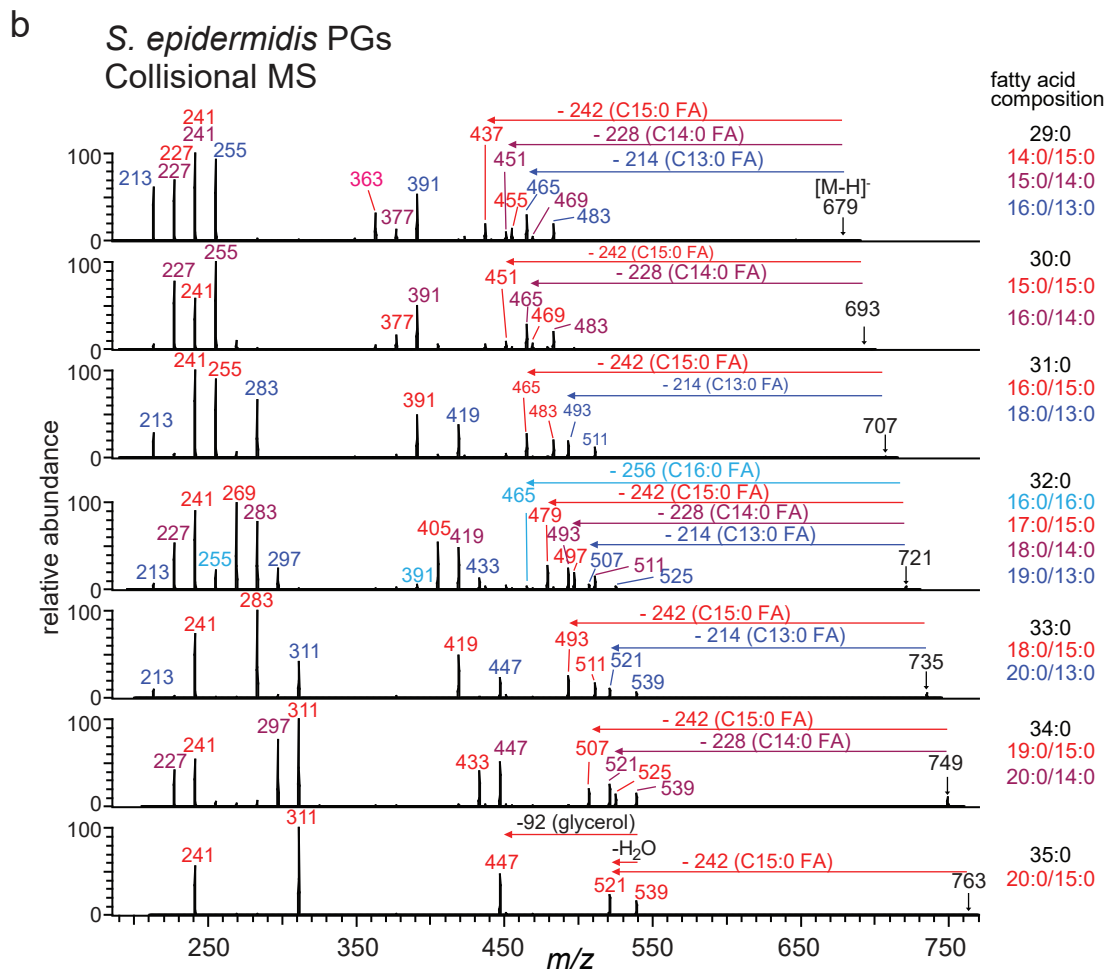
(a) Gating strategies used to identify and quantify CD1a-tetramer⁺ T cells included a lymphocyte gate - single cells - live, CD14-/CD19- - CD3+ T cells - tetramer gate. For the tetramer gate we have used a gate that was more stringent than FMO. This gate was empirically established by sorting low (mfi < 10³) and high tetramer staining cells and validating whether they are truly CD1a tetramer specific. This stringent gate was used for all T cell sorts as well as the ex vivo data depicted in Figures 1e, 1f, 1g, 2a, 5, 6e. In later tetramer experiments, we washed CD1a monomers after lipid loading to remove detergent and excess lipid. This step significantly reduced non-specific staining and allowed us to use the less stringent FMO gate (b). This gate was used in Figure 6f.



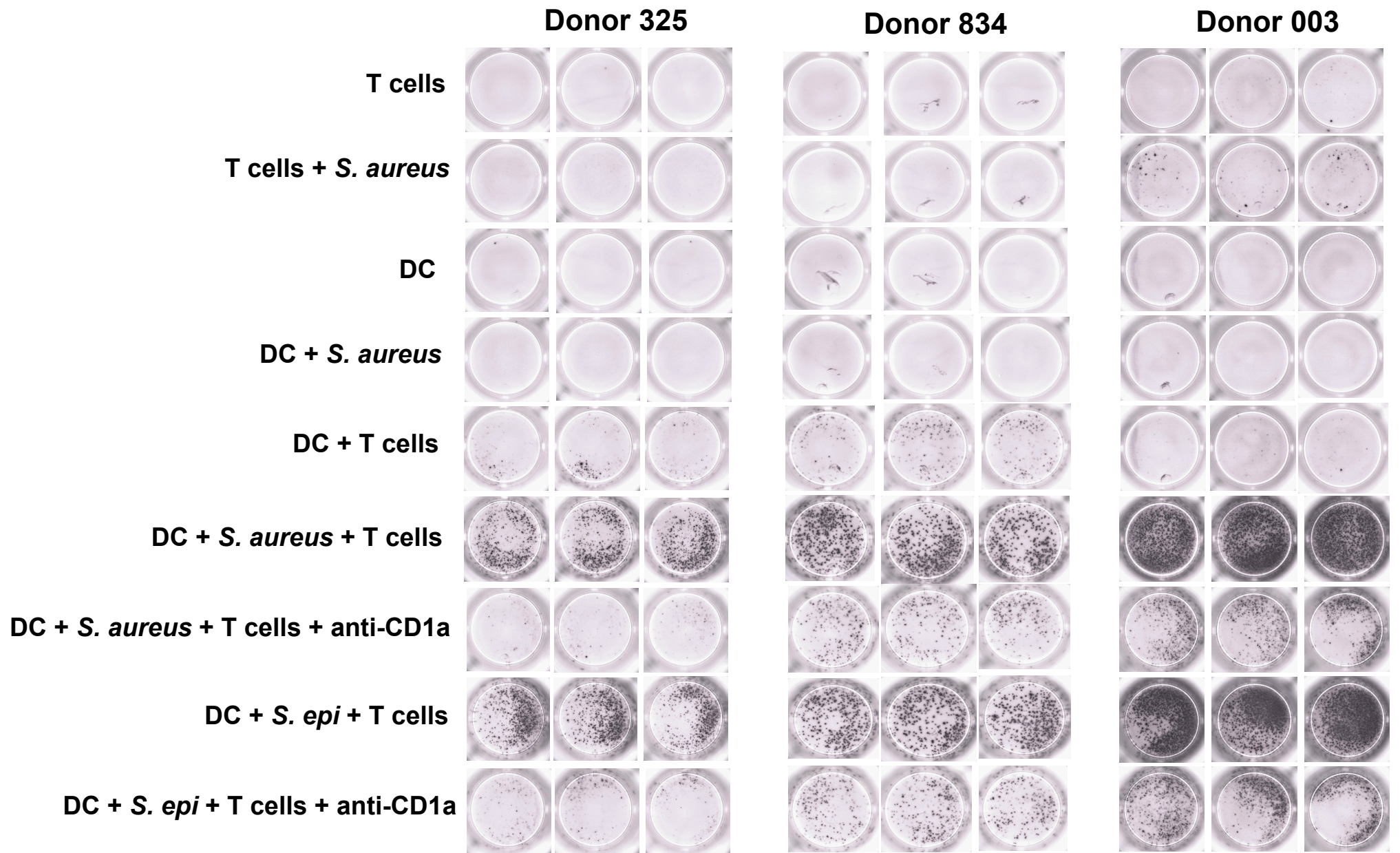
Supplementary Figure 2. UMAP projection of the tetramer-negative and CD1a-(lysyl)PG tetramer+ CD4+ T cells colored by donor, corresponding to the UMAP plots of main Figure 5a.



Supplementary Figure 3. Violin plots depicting normalized expression values of indicated genes from single cell RNA-seq data (main Figure 5) of tetramer-negative and CD1a-(lysyl)PG tetramer+ CD4+ T cells. The clusters correspond to the clusters in the UMAP plots and heatmap of Figure 5.



IL-13 Elispot tetramer-sorted CD4+ T cells with dendritic cell (DC) and bacterial co-culture



Supplementary Figure 5.

IL-13 Elispot of tetramer+ CD4+ T cells that were FACS-sorted from polyclonal CD1a-(lysyl)PG tetramer+ T cell lines. (Figure 6c) Co-culture conditions (triplicates) are indicated on the left.

Supplementary Table 1

T cell polyclonal cultures / lines / clones reported in manuscript

Donors	Origin	T cell lines (low and high purity)	T cell clones	TCR identified	Experiments with Donor / T cell lines / clones	Figure(s)	IL-13 production
DermT (reference 17, 18)	Skin (dermis)	DermT			Tetramer stainings / sort Functional assays (K562 CD1a)	1b, 1c, EDFig 1 1a	
834	PBMC	834			Tetramer stainings / sort Dual tetramer staining Cytokine qPCR (with T cell line) Co-culture assay (DC + S. aureus)	2a, EDFig 8 3e 4d 6c, EDFig 7, S5	+
350	PBMC	350	305.2	-	Tetramer stainings / sort	2a, 2c (clone)	+
325	PBMC	325			Tetramer stainings / sort Functional assay (K562 CD1a + lipid) Cytokine qPCR (after ex vivo sort from PBMC) Single cell RNA-seq after ex vivo sort from PBMC Co-culture assay (DC + S. aureus)	2a, EDFig 8 2e 4c 5a - 5e 6c, EDFig 7, S5	+
213	PBMC	213			Tetramer stainings / sort	2a, 2b	+
003	PBMC	003	multiple	-	Tetramer stainings / sort Co-culture assay (DC + S. aureus)	2a 6c, EDFig 7, S5	+
966	PBMC	966	966.10 (CD4+) 966.1.4- (CD4-) 966.1.4+ (CD4+)	966.10	Tetramer stainings / sort Functional assay (K562 CD1a + lipid) Dual tetramer staining Bulk RNA-sequencing Intracellular cytokine staining (ICS)	2a, 3c 2e 3e 4a 4b	+
921	PBMC	921a (MACS/FACS sort) 921b (FACS sort)	921.3 (CD4+) 921.2 (CD4+)	921.3, 921.2	Tetramer stainings / sort Functional assay (Plate-bound CD1a + lipid) Surface Plasmon Resonance (TCR clone 921.3) Bulk RNA-sequencing Intracellular cytokine staining (ICS) Single cell RNA-seq after ex vivo sort from PBMC	2a, 2b, 2c, 3b, EDFig 8 2d 3d 4a 4b 5a-5e	+
2114 (BC14)	PBMC	2114 (MACS/FACS sort)	2114.1, 2114.5, 2114.8	2114.8	Tetramer stainings / sort Functional assay (K562 CD1a + lipid)	2c, 3c 2e	+
SkinT4	Skin	SkinT4	SkinT4.1	SkinT4.1	Tetramer stainings / sort Functional assay (Plate-bound CD1a + lipid)	6d 6d	+
211	PBMC	211			CD1a-PG sort and dual tetramer staining	EDFig 4	not tested
773	PBMC				Cytokine qPCR (after ex vivo sort from PBMC)	4c	+
678, 689, 262, 715	PBMC				Ex vivo dual tetramer staining	3f	
211, 671, 670, 182, 678, 679	PBMC				Ex vivo tetramer staining	1g	
ADE001 - ADE019	PBMC				Ex vivo tetramer staining	6e	
ADE001 - ADE019	Skin biopsies				In vitro tetramer staining	6e	
Oxford samples	PBMC				Ex vivo tetramer staining	6f	

Supplementary Notes

Fatty acid methyl ester (FAME) preparation and HPLC-MS analysis.

Lipid standards were purchased from Nui-chek Prep (straight chain, n-C15 FAME, (N-15-A) and Avanti Polar Lipids (anteiso-C15:0 fatty acid, 857510; iso-C15:0 fatty acid, 857511). Fatty acid methyl esters were prepared using the published method.¹ Anteiso-C15:0 fatty acid (200 µg), iso-C15:0 fatty acid (200 µg), and purified *S. aureus* PGs (25 µg) were subject to FAME conversion. Briefly, lipids were dried in 15-ml glass tubes and 2 ml of 5% methanolic (m/v) HCl was added and heated at 80 °C in a water bath for 2 hours. The solution was cooled down to the 20-25°C and 1 ml water was added, followed by 2 ml of hexane with vortexing for 30 seconds for each solvent addition. The tubes were centrifuged at 2500 rpm for 10 min, and the FAME-containing upper phase was transferred to a clean tube and dried under nitrogen gas. For the reversed phase HPLC-QTOF-MS analysis, the *S. aureus* FAME corresponding to 1 µg of initial input PGs was used to compare the three FAME (n-, iso-, and anteiso-C15 FAME) standards (10 µM) using HPLC-MS system described for PG and lysylPG analysis.

1D TLC purification for *S. aureus* PG and lysylPG.

For PG and lysylPG isolation, 1 ml of frozen *S. aureus* pellet was thawed and extracted by the Bligh and Dyer method². Silica-coated glass TLC plates (Sorbtech, 2115026; 20 x 20 cm, 250 µM) were precleared by chloroform/methanol/water (60:30:6 (v/v/v)). The *S. aureus* lipids extract was loaded on the TLC plate (1 mg per plate for two plates) and developed with C/M/H₂O 65/25/4 (v/v/v) and dried for 1 hr³. Plates were separated to two pieces in a ratio of 8:2, with the small piece was sprayed with the solution of 3% (m/v) of cupric acetate in 8% (v/v) phosphoric acid, and the lipid bands were visualized after charring for 20–30 min at 150°C. PGs have a retention factor (R_f) of ~0.26-0.30 and lysylPGs have an R_f ~0.05-0.09. Based on the reference bands on the small TLC piece, the PG and lysylPG containing bands on the large TLC piece were marked

and scraped. The silica was extracted twice with C/M (2:1; v/v). The lysylPG fraction was dried for the final analysis without further purification to avoid lysine head group hydrolysis. The PG fraction contained trace cardiolipins due to their similar R_f as detected of ESI-MS. To remove cardiolipin, the fraction was further purified using the reversed phase HPLC system described above and monitored by a QTOF mass spectrometer. The HPLC column was diverted at the known PG elution time and the eluate was collected in a glass tube. Twenty HPLC column purifications were made from one 1D TLC plate purified PGs to yield pure PG as assessed by ESI-MS. Purified lipids were quantified based on the PG and lysylPG external standard curves as described in the lysylPG stability test section.

Bulk RNA-sequencing of CD1a-lysylPG tetramer+ CD4+ T cells

Purified tetramer+ cells were incubated with or without anti-CD3/CD28 stimulator beads (stimulated) (Dynabeads[®] Human T-activator CD3/CD28) for 6 hours, after which RNA was extracted using RNeasy (Qiagen). RNA Library Preparation and HiSeq Sequencing RNA sample was quantified using Qubit 2.0 Fluorometer (Life Technologies). RNA integrity was checked with 2100 Bioanalyzer (Agilent Technologies). RNA library preparation and sequencing reaction were conducted at GENEWIZ, LLC. RNA sequencing library preparation used the NEBNext Ultra RNA Library Prep Kit for Illumina by following manufacturer's recommendations (NEB). Briefly, mRNA was first enriched with Oligod(T) beads. Enriched mRNAs were fragmented for 15 minutes at 94 °C. First strand and second strand cDNA were subsequently synthesized. cDNA fragments were end repaired and adenylated at 3'ends, and universal adapter was ligated to cDNA fragments, followed by index addition and library enrichment with limited cycle PCR. The sequencing library was validated on the Agilent 2100 Bioanalyzer (Agilent Technologies), and quantified by using Qubit 2.0 Fluorometer (Invitrogen) as well as by quantitative PCR (Applied Biosystems). The

sequencing library was clustered on one lane of a flowcell. After clustering, the flowcell was loaded on the Illumina HiSeq instrument according to manufacturer's instructions. The samples were sequenced using a 2x150 Paired End (PE) configuration. Image analysis and base calling were conducted by the HiSeq Control Software (HCS). Raw sequence data (.bcl files) generated from Illumina HiSeq was converted into fastq files and de-multiplexed using Illumina's bcl2fastq 2.17 software. One mis-match was allowed for index sequence identification. Unique gene hit counts were calculated by using feature Counts from the Subread package v.1.5.2. Only unique reads that fell within exon regions were counted. After extraction of gene hit counts, the gene hit counts table was used for downstream differential expression analysis. Variance-stabilizing transformation (VST) was performed, and the VST data of cytokine and chemokine expression was displayed in a heatmap using Morpheus (<https://software.broadinstitute.org/morpheus/>).

Cytokine ELISA and Elispot

Nunc Maxisorp 96-well plates (ThermoFisher, 439454) were coated at 4°C overnight with 50µl of 5µg/ml of antibody in PBS. Next, plates were washed and blocked with 300µl of 1% BSA in PBS at 20-25°C for 1 hour. Samples and standard curve dilutions were added to the plate in triplicate and incubated at 20-25°C for 2 hours. After washing, 50µl of biotin-tagged antibody at 0.5 µg/ml in PBS was added and incubated for 1 hour at 20-25°C. Plates were washed again before the addition of streptavidin-HRP diluted 1:1000 in PBS, for 30 minutes at 20-25°C. Plates were washed again before the addition of 50µl of hydrogen peroxide and tetramethylbenzidine (R&D Systems, DY999). The reaction was stopped with 25µl H₂SO₄.

ELISA sandwich antibody pairs: GM-CSF antibody pairs (Thermo Fisher Scientific, M501B & M500A); IFN γ (Mabtech, 3420-3-250 & 3420-6-250); IL-13 (Mabtech, 3471-3-250, 3471-6-250).

Cytokine ELISAs were performed according to manufacturer's instruction (Mabtech).

References

1. Hassan, N. *et al.* Temperature Driven Membrane Lipid Adaptation in Glacial Psychrophilic Bacteria. *Frontiers in microbiology* **11**, 824 (2020).
2. Bligh, E.G. & Dyer, W.J. A rapid method of total lipid extraction and purification. *Canadian journal of biochemistry and physiology* **37**, 911-917 (1959).
3. Peschel, A. *et al.* Staphylococcus aureus resistance to human defensins and evasion of neutrophil killing via the novel virulence factor MprF is based on modification of membrane lipids with l-lysine. *The Journal of experimental medicine* **193**, 1067-1076 (2001).